Available online at www.sciencedirect.com
ScienceDirect
Journal of Sound and Vibration 298 (2006) 180–193
JOURNAL OF SOUND AND VIBRATION
www.elsevier.com/locate/jsvi

# Optimization of electromechanical control of beam dynamics: Analytical method and finite differences simulation

C.A. Kitio Kwuimy[a], B.R. Nana Nbendjo[a], P. Woafo[b,*]

[a]Laboratory of Mechanics, Faculty of Science, University of Yaounde I, Box 812, Yaounde, Cameroon
[b]Laboratory of Nonlinear Modeling and Simulation in Engineering and Biological Physics, University of Yaounde I, Box 812, Yaounde, Cameroon

Received 27 January 2005; received in revised form 8 May 2006; accepted 9 May 2006
Available online 18 July 2006

**Abstract**

This paper deals with the optimization of the electromechanical control of beams dynamics. Using the mode expansion formalism, an analytical investigation is carried out to find adequate electrical parameters to reduce the vibration amplitude, to control the snap through instability and horseshoe chaos. The analytical investigation is validated and complemented by the numerical simulation of the modal equations as well as by the direct numerical simulation of the beam nonlinear partial differential equation under control.


## 1. Introduction

Recent years have witnessed a growing interest in the wish to control vibration in linear and nonlinear systems. In this line, many works have been devoted to the dynamic vibration absorber [1–7]. This is used to reduce excessive vibration in mechanical structures. Nagem et al. [8] studied the control of a linear structure subject to an electromechanical control and found that, with a good choice of parameters the amplitude of the system can be reduced. Nana et al. [9,10] presented a process of optimizing the control devices focussing their attention on a single- and double-well Duffing oscillator with delay and concluded that control can turn in bad or good direction depending on the values of the control gain parameters. Moreover, the time-delay has strong effect on the value of the critical parameters leading to control.

All these works have been done by considering a set of ordinary differential equations approximating the nonlinear partial differential equations of the structure. In the case of beams, the modal equations are obtained when one applies approximation methods such as Galerkin method or Fourier series. Thus, there is a real interest to complement and compare the results of the modal analysis to that of a direct numerical simulation of the full nonlinear partial differential equation of the beam dynamics. This is the main aim of this paper containing five sections. Section 2 considers the structural model, its equations and the discretization scheme to solve the partial differential equation. Section 3 deals with the derivation of the parameters leading

*Corresponding author.
*E-mail address:* pwoafo@uycdc.uninet.cm (P. Woafo).

0022-460X/$ - see front matter © 2006 Elsevier Ltd. All rights reserved.
doi:10.1016/j.jsv.2006.05.019

to the reduction of the amplitude of vibration. Section 4 is devoted to the effects of the controller on the Melnikov chaos and snap-through instability. At each step, the results of both the modal equations analysis and that of the numerical simulation of the partial differential equations are given. Section 5 concludes the paper.

## 2. Physical system, equations and numerical scheme

### 2.1. Physical system

Consider an electromechanical controlled beam of length $L_1$ under a localized periodic force as shown in Fig. 1. In discussing beams, attention is restricted to planar and non-rotating motion. Assuming that each section remains in its plane and considering a linear stress strain law, the equations of motion governing the nonlinear dynamics of a beam with uniform shape subject to a localized periodic load of intensity $f_1$ and frequency $w$ under the electromechanical control (Fig. 1) are given as [11]

$$\rho A\frac{\partial^2 U}{\partial \tau^2}-EA\frac{\partial^2 U}{\partial X^2}=\frac{EA}{2}\frac{\partial}{\partial X}\left[\left(1-2\frac{\partial U}{\partial X}\right)\left(\frac{\partial V}{\partial X}\right)^2\right], \tag{1}$$

$$\rho A\frac{\partial^2 V}{\partial \tau^2}+P\frac{\partial^2 V}{\partial X^2}+EJ\frac{\partial^4 V}{\partial X^4}+2\eta\frac{\partial V}{\partial \tau}=f_1\delta(X-X_0)\cos(\Omega\tau)+EA\frac{\partial}{\partial X}\left(e\frac{\partial V}{\partial X}\right)-l_bBi_0\delta(X-X_1), \tag{2}$$

$$e=\frac{\partial U}{\partial X}+\frac{1}{2}\left(\frac{\partial V}{\partial X}\right)^2-\left(\frac{\partial U}{\partial X}\right)^2. \tag{3}$$

The electric control device is described by

$$L_0\frac{\mathrm{d}i_0}{\mathrm{d}\tau}+R_0i_0=l_bB\frac{\partial V}{\partial \tau}\delta(X-X_1). \tag{4}$$

In Eqs. (1) and (2), $E$ is the Young modulus of the beam, $\rho$ is the beam density, $A$ and $J$ are, respectively, the area and the moment of inertia of the beam cross-section of radius of gyration $r_0$, $V(X,\tau)$ is the transversal deflection of the beam while $U(X,\tau)$ is the axial displacement, $V$ and $U$ depend on the spatial coordinate $X$ and time $\tau$, $\delta(.)$ stands for Dirac delta function and $f_1\delta(X-X_0)\cos(\Omega\tau)$ is the periodic force, $\eta$ is the damping which is assumed to be constant, $P$ is the constant axial force, $L_0$ and $R_0$ are, respectively, the inductance and resistance of the control device, $X_0$ and $X_1$ are the positions of the localized force and the control device.

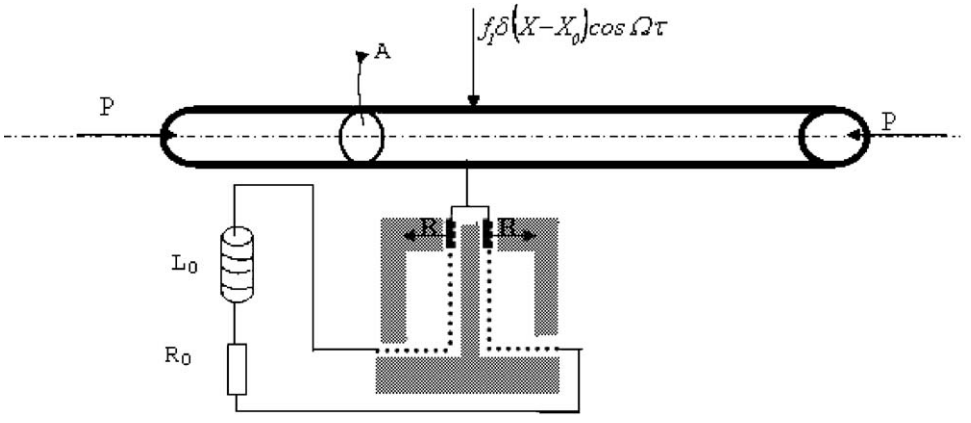


Fig. 1. Beam under electromechanical control.

We introduce the dimensionless variables:

$$x=\frac{X}{L_1},\quad u=\frac{U}{L_1},\quad v=\frac{V}{L_1},\quad r=\frac{r_0}{L_1},\quad T_0=\frac{L_1^2}{r_0}\sqrt{\frac{\rho}{E}},\quad \lambda=\frac{L_1^2\eta}{r_0EA}\sqrt{\frac{E}{\rho}},\quad \omega=\Omega T_0,$$

$$f=\frac{f_1L_1}{EA},\quad t=\frac{\tau}{T_0},\quad L=\frac{L_0I_0}{T_0U_0},\quad R=\frac{R_0I_0}{U_0},\quad f_{22}=\frac{Bl_bl}{T_0U_0},\quad f_{11}=\frac{Bl_bI_0}{EA},\quad \Gamma=\frac{PL_1^2}{r^2EA},$$

and

$$i_1=\frac{i_0}{I_0}.$$

Here $U_0$ and $I_0$ are, respectively, the characteristic voltage and current of the electromechanical device. Consider a hinged–hinged beam and assume that the longitudinal inertial term $r^2\partial^2u/\partial t^2$ and $(\partial u/\partial x)^2$ are negligible (case of beam with small radius of gyration $r$), Eqs. (1)–(4) reduce to

$$r^2\left(\frac{\partial^2v}{\partial t^2}+2\lambda\frac{\partial v}{\partial t}+\frac{\partial^4v}{\partial x^4}+\Gamma\frac{\partial^2v}{\partial x^2}\right)=e\frac{\partial^2v}{\partial x^2}+f\delta(x-x_0)\cos(wt)-f_{11}i_1\delta(x-x_1) \tag{5}$$

$$L\frac{\mathrm{d}i_1}{\mathrm{d}t}+Ri_1=f_{22}\frac{\partial v}{\partial t}\delta(x-x_1) \tag{6}$$

with $e=(1/2)\int_0^1(\partial v/\partial x)^2\,\mathrm{d}x$. Throughout the paper, we use $r=0.04$, $f=0.04$ (otherwise indicated) and $\lambda=0.4$. We will assume $f_{11}=f_{22}$.

### 2.2. Mode equations

For the analytical purpose, it is convenient to assume an expansion of the deflection $v(x,t)$ in terms of the combination of the linear free oscillation modes, which are those of a hinged–hinged beam in this case. Thus, one can write $v(x,t)$ in the form

$$v(x,t)=\sum_{m=1}^{\infty}q_m(t)\Phi_m(x), \tag{7}$$

where $\Phi_m$ are the eigenfunctions of the equation

$$\frac{\partial^2v}{\partial t^2}+\frac{\partial^4v}{\partial x^4}=0 \tag{8}$$

with the boundary conditions

$$v(0,t)=0,\quad \left(\frac{\partial^2v}{\partial x^2}\right)(0,t)=0,\quad v(1,t)=0,\quad \left(\frac{\partial^2v}{\partial x^2}\right)(1,t)=0, \tag{9}$$

and $q_m$ are dynamical functions to be determined. $\Phi_m$ are thus defined as $\Phi_m(x)=\sin(m\pi x)$. Substituting Eq. (7) into Eqs. (5) and (6), multiplying Eq. (5) by $\Phi_m(x)$ and integrating over the dimensionless length $[0;1]$ of the beam leads to the modes equations

$$\frac{\mathrm{d}^2q_n}{\mathrm{d}t^2}+2\lambda\frac{\mathrm{d}q_n}{\mathrm{d}t}+[w_{0n}^2+a_n]q_n=f_n\cos(wt)-g_ni_1, \tag{10}$$

$$L\frac{\mathrm{d}i_1}{\mathrm{d}t}+Ri_1=\sum_{m=1}^{\infty}h_m\frac{\mathrm{d}q_m}{\mathrm{d}t} \tag{11}$$

with

$$g_n=\frac{2f_1\sin(n\pi x_1)}{r^2},\quad w_{0n}^2=(n\pi)^2((n\pi)^2-\Gamma),\quad a_n=\left(\frac{n\pi}{4r}\right)^2\sum_{m=1}^{\infty}(mq_m)^2,$$

$$f_n = \frac{2f}{r^2}\sin(n\pi x_0), \quad h_m = f_2 \sin m\pi x_1.$$

Around the $n$th mode, this set of equations becomes

$$\frac{d^2 q_n}{dt^2} + 2\lambda \frac{dq_n}{dt} + (w_{0n}^2 + b_n)q_n = f_n \cos wt - g_n i_1, \tag{12}$$

$$L\frac{di_1}{dt} + Ri_1 = h_n \frac{dq_n}{dt} \tag{13}$$

with

$$b_n = \frac{(n\pi)^4}{4r^2}.$$

From Eq. (12), the one mode dynamics of the beam is that of a Duffing like oscillator with a one well potential (hard Duffing oscillator) if $\Gamma > n^2\pi^2$ and a two wells potential if $\Gamma < n^2\pi^2$. In the first configuration, the dynamics shows nonlinear vibration around the equilibrium state of the beam and also chaotic dynamics for large value of the transversal load. Since an analytical prediction of chaos is not possible in this case, we restrict the analysis to the control of vibration amplitude. This is done in Section 3. In the second case, two particular behaviors can be found: snap-through instability and horseshoe or Melnikov chaos. In Section 4, we derive the parameters to control these two types of behavior which are dangerous for mechanical structures.

### 2.3. The direct numerical scheme

To solve numerically Eqs. (5) and (6), we set $h = 1/N$, $x = (i-1)h$ and $t = jk$ where $h$ and $k$ are the spatial and temporal steps, $i$ and $j$ are integer variables relative to position and time and $N$ is the number of discrete points considered along the beam length. The finite differences definition and trapeze formula transform the partial differential equations into

$$v_{i,j+1} = \frac{1}{A_1}\left[\frac{f\delta[h(i-1)-x_0]\sin(wt) - f_1 i_{1j}\delta[h(i-1)-x_1]}{r^2} - A_2 v_{i,j} - A_3(v_{i+1,j} - v_{i-1,j}) - A_4(v_{i+2,j} - v_{i-2,j}) - A_5 v_{i,j-1}\right], \tag{14}$$

$$i_{1j+1} = i_{1j-1} + \frac{f_2(v_{i,j+1} - v_{i,j-1})\delta[h(i-1)-x_1] - 2KRi_{1j}}{L}, \tag{15}$$

where

$$A_1 = \frac{1}{k^2} + \frac{\lambda}{2k}, \quad A_2 = \frac{-1}{k^2} + \frac{6}{h^4} + \frac{2(\Gamma - \mathrm{tr})}{h^2}, \quad A_3 = -\frac{4}{h^4} + \frac{\mathrm{tr} - \Gamma}{h^2}, \quad A_4 = \frac{1}{h^4},$$
$$A_5 = \frac{1}{k^2} - \frac{\lambda}{2k} \quad \text{and} \quad \mathrm{tr} = \frac{1}{16r^2h}\left[4(v_{2,j})^2 + (v_{n,j})^2 + 2\sum_{i=2}^{n}(v_{i+1,j} - v_{i-1,j})^2\right].$$

The boundary conditions are

$$v_{1,j} = v_{n+1,j} = 0, \quad v_{n+2,j} = -v_{n,j}, \quad v_{0,j} = -v_{2,j} \quad \forall j. \tag{16}$$

This discretization scheme is stable if

$$\frac{8}{h^4} \leqslant \frac{1}{k^2}\left[1 + \sqrt{1 - \frac{(\lambda k)^2}{4}}\right] \tag{17}$$

with $\lambda k \leqslant 2$.

## 3. Optimization of the electromechanical control of vibration in a single-well potential

In this section we set $\Gamma = 0$ (beam with no axial load). To determine the amplitude of harmonic vibrations of the system under control, we use the harmonic balance method. In this spirit, we set

$$q_n(t) = \gamma_n \cos(wt + \phi_n). \tag{18}$$

Inserting this expression in Eqs. (12) and (13) then equating the coefficient of $\sin(wt)$ and $\cos(wt)$, we find that the amplitude $\gamma_n$ obeys the following nonlinear algebraic equation

$$\gamma_n^2\left(w_{0n}^2 - w^2 + 3\left(\frac{n^2\pi^2}{4r}\right)^2\gamma_n^2 + \frac{Lw^2k_n}{(Lw)^2 + R^2}\right)^2 + \left(2\lambda w + \frac{Rwk_n}{(Lw)^2 + R^2}\right)^2 = f_n^2 \tag{19}$$

with

$$k_n = \frac{f_{11}f_{22}}{r^2}\sin(n\pi x_1).$$

For the beam without control, the amplitude of vibration satisfies the following equation:

$$A_n^2\left[\left(w_{0n}^2 - w^2 + 3\left(\frac{n^2\pi^2}{4r}\right)^2 A_n^2\right)^2 + (2\lambda w)^2\right] = f_n^2. \tag{20}$$

The control strategy is effective when the amplitude of the system with the electromechanical device is less than that of the uncontrolled system, that is $\gamma_n \leqslant A_n$. Let us first assume that the nonlinear term $b_n q_n^3$ is negligible.The controlling device is efficient when

$$L \leqslant \frac{4R\lambda + k_n}{2(w^2 - w_{0n}^2)}. \tag{21}$$

In the $(w, L)$ plane, this requires that

$$R < \frac{-k_n}{4\lambda} \quad \text{for } w < w_{0n} \tag{22}$$

and

$$R > \frac{-k_n}{4\lambda} \quad \text{for } w > w_{0n}. \tag{23}$$

In Fig. 2 we have plotted relation (21) in the $(w, L)$ plane for condition (22) (curve with line). The results of the finite differences simulation of Eqs. (14) and (15) are also reported (dotted line). There is a fairly good agreement with the analytical result (thin line) around the natural frequency of the first mode $n = 1$ (Fig. 2a). The same remark is made as the external frequency is greater than the natural frequency of the third mode (Fig. 2b). The domain located below the curve is where the control is effective in reducing the amplitude of vibration. The boundary $R(w)$ for the control is also presented (Fig. 3) assuming that $w > w_{cn}$ with

$$w_{cn} = \sqrt{\frac{k_n}{2L} + w_{0n}^2}.$$

The domain located above the curve is where the control is effective in reducing the amplitude of vibration around the natural frequency of the first (Fig. 3a) and third modes (Fig. 3b).

For the nonlinear case (the term $b_n q_n^3$ taken into account), we proceed as follows. The boundary condition is obtained by setting

$$A_n = \gamma_n. \tag{24}$$

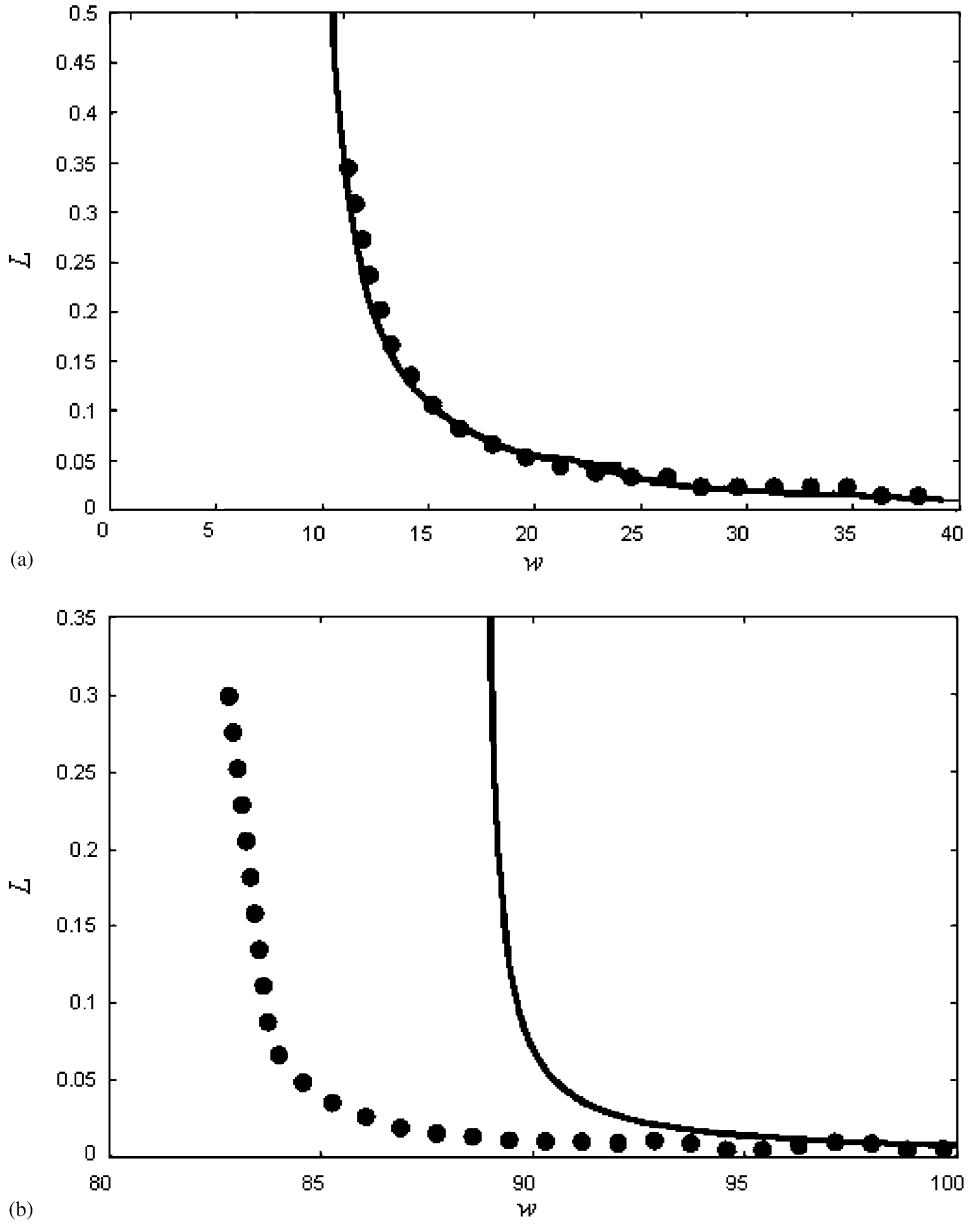


Fig. 2. Boundary of controlled domain in $(w, L)$ plane for $R = 20, f_{11} = 0.01$ in the case of linear dynamics: (a) around the first natural frequency and (b) around the third natural frequency.

Using Eqs. (19) and (20), the amplitude at the boundary is given by

$$A_n = \gamma_n = \sqrt{\frac{4}{6Lb_n}\left[2L(w^2 - w_{0n}^2) - k_n - 4\lambda R\right]} \tag{25}$$

with

$$L \geqslant \frac{k_n + 4\lambda R}{2(w^2 - w_{0n}^2)}. \tag{26}$$

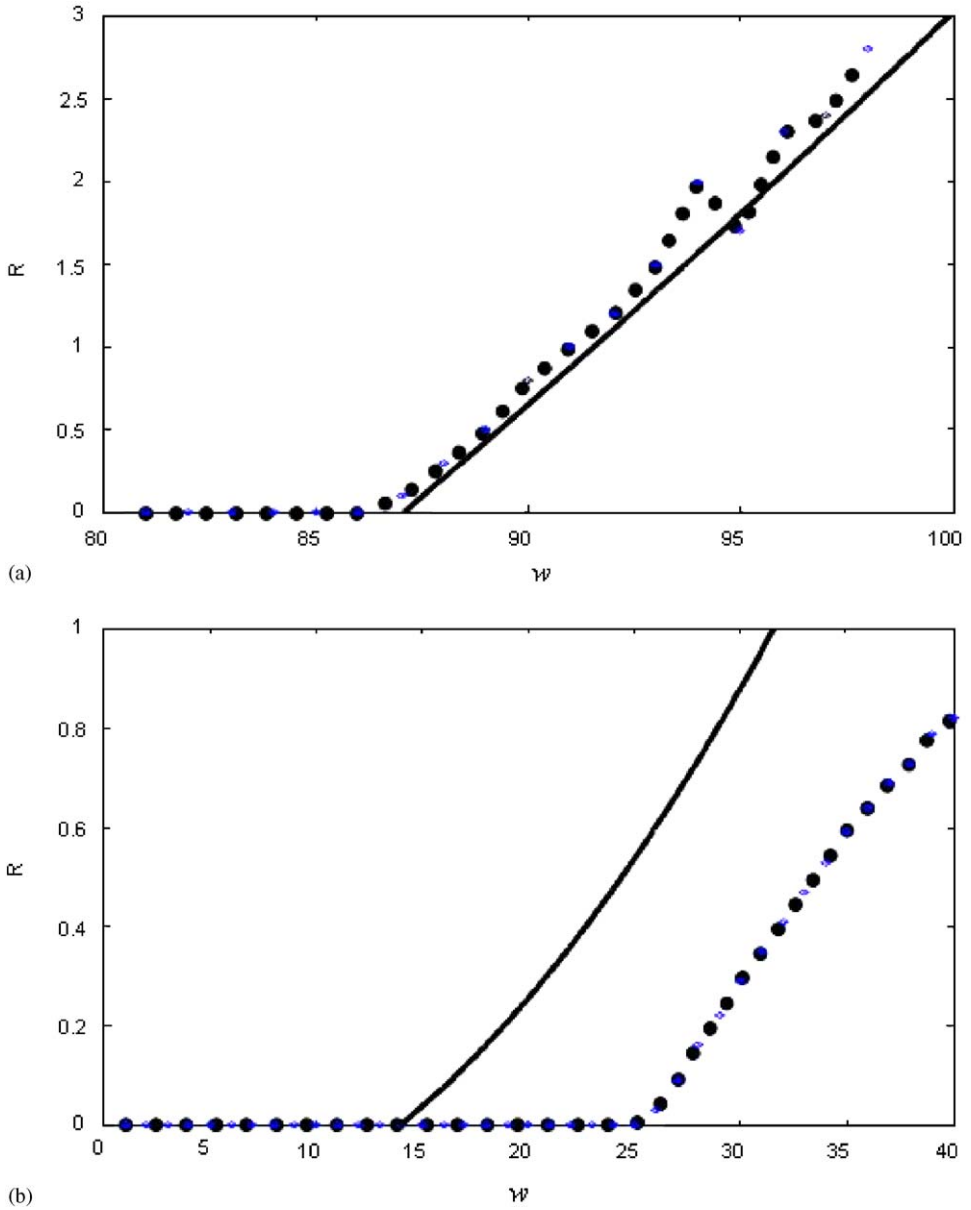


Fig. 3. Boundary of controlled domain in $(w, R)$ plane for $L = 0.01, f_{11} = 0.01$ in the case of linear dynamics: (a) around the first natural frequency and (b) around the third natural frequency.

Inserting this expression (25) in Eq. (19) leads to

$$\frac{3b_n f_n^2}{4} = \left[w^2 - w_{0n}^2 - \frac{k_n + 4\lambda R}{2L}\right]\left[\left(\frac{k_n + 4\lambda R}{2L}\right)^2 + (2\lambda w)^2\right]. \tag{27}$$

This last equation defines in the parameters space the boundary for the efficiency of the control of the amplitude of vibration. It is plotted in Fig. 4. The agreement between the numerical results (dotted lines) and the analytical ones is better around the first mode than around the third mode.

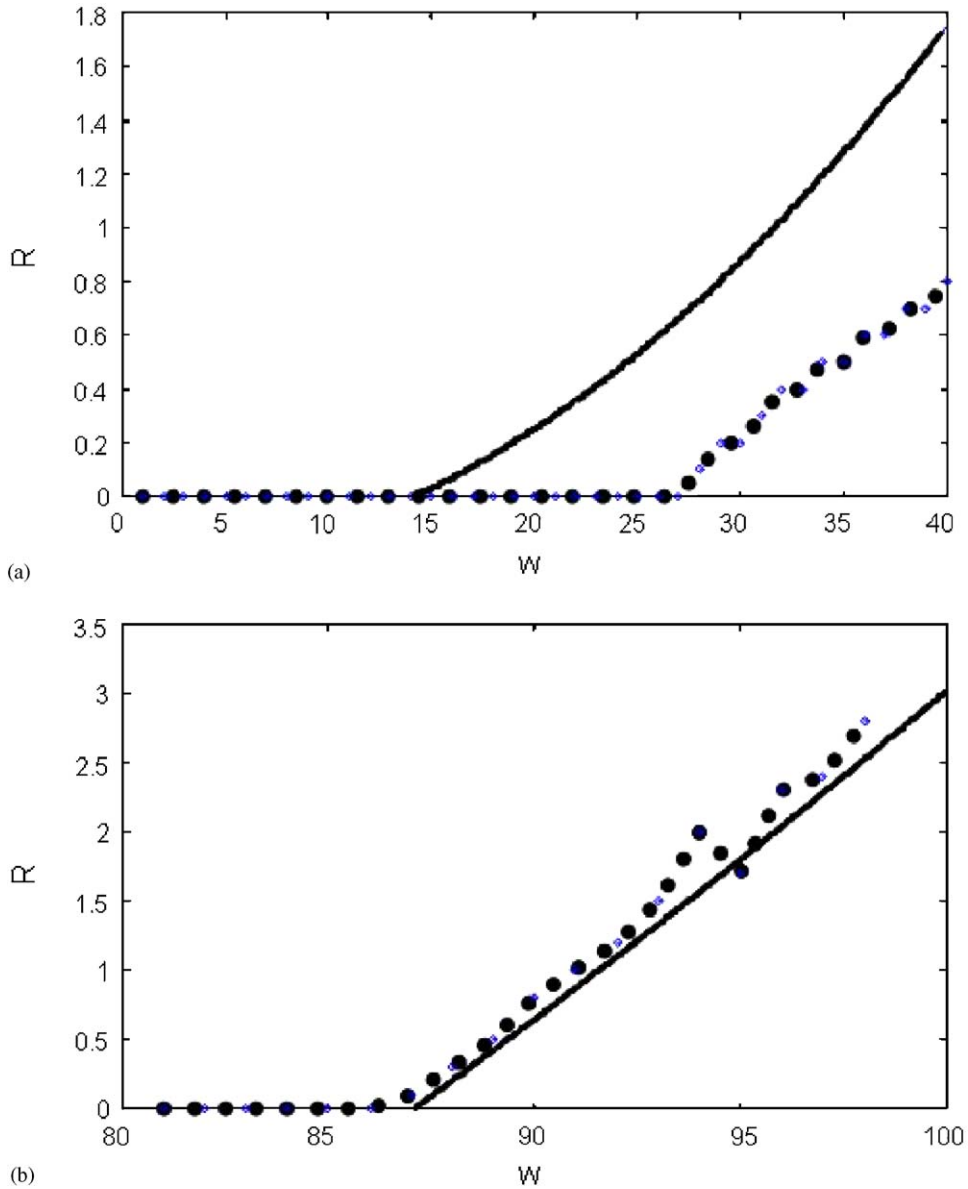


Fig. 4. Boundary of controlled domain in $(w, R)$ plane for $L = 0.01, f_{11} = 0.01$ and $f = 10^{-3}$ in the case of nonlinear dynamics: (a) around the first natural frequency and (b) around the third natural frequency.

## 4. Control of snap-through instability and Melnikov chaos in a double-well potential

### 4.1. Control of snap-through instability

In this section we set $\Gamma = 10.88$ and we consider the first mode ($n = 1$) for analytical investigation. The structure thus possesses a double-well configuration. In a double-well potential, the structure often changes the sign of its curvature. This is called snap-through instability. Analytically, the critical value $f_{1\mathrm{cr}}$ of the external load can be computed from the fact that snap-through instability occurs when the structure initially at the stable point $q_{01s} = \pm 2r/\pi\sqrt{\Gamma - \pi^2}$ crosses the potential barrier at $q_{01i} = 0$. The snap-through instability

takes place if $f_1 > f_{1cr}$. To derive the expression of $f_{1cr}$, we set

$$q_n = A_{0n} + A_n \cos(wt + \phi_n). \tag{28}$$

Inserting this expression in Eqs. (12, 13) and considering the crossing condition, we obtain

$$\left(-w_{01}^2 - w^2 + \frac{Lw^2k_1}{(Lw)^2 + R^2}\right)^2 + \left(2\lambda w + \frac{Rwk_1}{(Lw)^2 + R^2}\right)^2 = \frac{5b_1}{2w_{01}^2} f_{1cr}. \tag{29}$$

The variation of $f_{1cr}$ versus $w$ and $f_{11}$ is reported in Figs. 5 and 6 along with the results of the direct numerical simulation of Eqs. (14) and (15) and that of Eqs. (10) and (11). $f_{1cr}$ is an increasing function of $w$ and $f_{11}$.

### 4.2. Control of the horseshoe chaos

In Ref. [12], Holmes used the Melnikov theory [13] to derive in the parameters space the condition for the occurrence of horseshoe chaos in the bistable system studied in this paper. Later on, the condition of the parametric suppression of this type of chaos was established in Refs. [14,15]. Melnikov theory defines the condition for the appearance of the so-called transverse intersection points between the perturbed and unperturbed separatrices or the appearance of the fractality on the basin of attraction. Our interest here is to find how the parameters of the active control strategy affect the Melnikov condition for chaos or derive the range of the control parameters inhibiting the Melnikov or Smale-horseshoe chaos in the bistable system. To deal with such a problem, let us express the system of Eqs. (12) and (13) in the form (for $n = 1$)

$$\frac{dU}{dt} = F(U) + \varepsilon G(U, t), \tag{30}$$

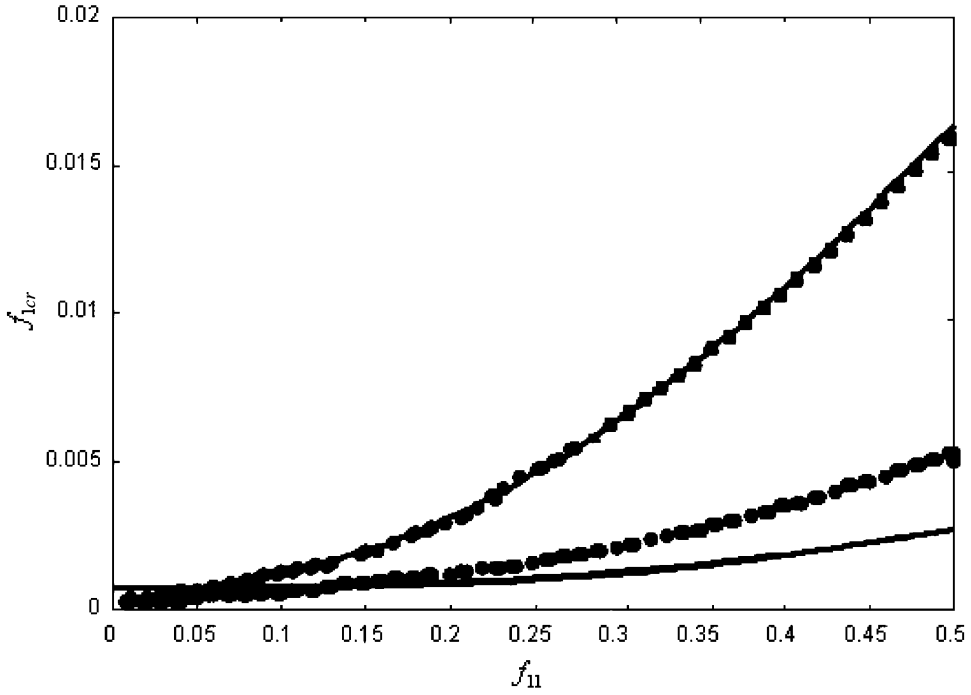


Fig. 5. The critical force $f_{1cr}$ for snap-through instability as function of $f_{11}$ for $w = 8$, $R = 20$, $L = 2 \times 10^{-3}$. Full lines: results of the analytical investigation. Line with crosses: results of the numerical simulation of the differential equations (12) and (13) with $n = 1$. Line with squares: results of the direct numerical simulation of the nonlinear partial differential equation.

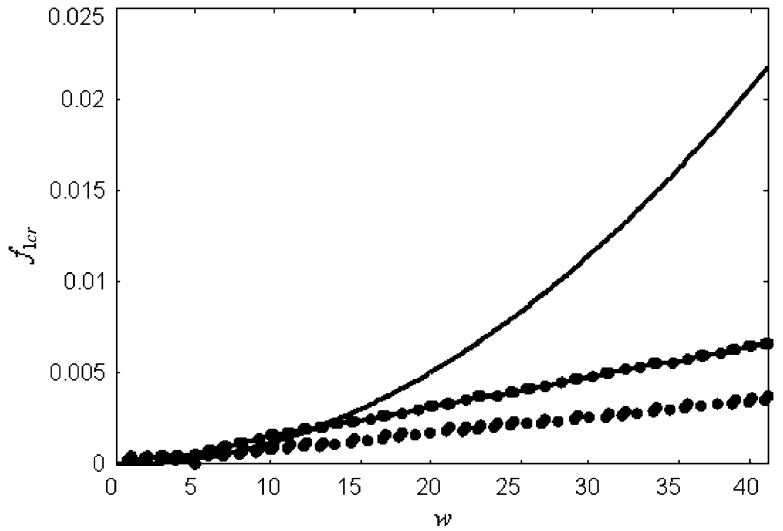


Fig. 6. The critical force $f_{1cr}$ for snap-through instability as function of $w$ for $f_{11} = 0.1$, $R = 20, L = 0.025$. Full lines: results of the analytical investigation. Crosses: results of the numerical simulation of the differential equations (12) and (13) with $n = 1$. Line with squares: results of the direct numerical simulation of the nonlinear partial differential equation.

where in the state vector notation

$$U = \left(q_1, p_1 = \frac{\mathrm{d}q_1}{\mathrm{d}t}\right), \quad F = (p_l, w_{01}^2 q_1 - b_1 q_1), \quad G = (0, -2\lambda p_1 - g_1 i_1 + f_1 \cos(wt)).$$

The unperturbed Hamiltonian system possesses two homoclinic orbits $U_0(t)$ connecting the unstable point $q_{01i} = 0$ of the potential to itself. These orbits are given by the following components:

$$q_0 = \pm\sqrt{\frac{2(-w_{01}^2)}{b_1}}\cosh^{-1}\left(\sqrt{-w_{01}^2}t\right), \tag{31}$$

$$p_0 = \mp\sqrt{\frac{2(-w_{01}^2)^2}{b_1}}\cosh^{-1}\left(\sqrt{-w_{01}^2}t\right)\ \tanh\left(\sqrt{-w_{01}^2}t\right) \tag{32}$$

and

$$i_{01} = \pm\frac{h_1}{L}\sqrt{\frac{2(-w_{01}^2)^2}{b_1}}\mathrm{e}^{-\alpha t}\int_0^t \mathrm{e}^{-\alpha s}\cosh^{-1}\left(\sqrt{-w_{01}^2}s\right)\ \tanh\left(\sqrt{-w_{01}^2}s\right)\mathrm{d}s \tag{33}$$

with $\alpha = R/L$. The dimensionless current $i_{10}$ is obtained by integrating the second part of Eq. (13) knowing $q_0$ and $p_0$.

The Melnikov function is defined by

$$M(t_0) = \int_{-\infty}^{\infty} F(U_0(t)) \times G(U_0(t), t + t_0)\,\mathrm{d}t, \tag{34}$$

where $t_0$ is a phase angle. Carrying out the integration, one finds that

$$M(t_0) = \frac{8\lambda(-w_{01}^2)^{3/2}}{3b_1} + \pi w f\left(\frac{2}{b_1}\right)^{1/2}\cosh^{-1}\left(\frac{\pi w}{2\sqrt{-w_{01}^2}}\right)\sin(wt_0) \pm f_{11}2k(\alpha), \tag{35}$$

where

$$k(\alpha) = \int_{-\infty}^{\infty} \xi(t) e^{-\alpha t} \cosh^{-1}\left(\sqrt{-w_{01}^2}\, t\right) \tanh\left(\sqrt{-w_{01}^2}\, t\right) dt \tag{36}$$

and

$$\xi(t) = 16\pi \sin^3(\pi x_1)(\Gamma - \pi^2)^2 \left( \int_0^t e^{-\alpha s} \cosh^{-1}\left(\sqrt{-w_{01}^2}\, s\right) \tanh\left(\sqrt{-w_{01}^2}\, s\right) ds \right). \tag{37}$$

Using the Melnikov criterion for the appearance of the intersection between the perturbed and the unperturbed separatrices [12], it comes that chaos is suppressed when

$$f_1 \leqslant f_{1cm} = \left( \frac{8\lambda(-w_{01}^2)^{3/2}}{3b_1} \pm f_{11} 2k(\alpha) \right) \left( \pi r w \sqrt{\frac{2}{b_1}} \right)^{-1} \coth\left( \frac{\pi w}{2\sqrt{-w_{01}^2}} \right), \tag{38}$$

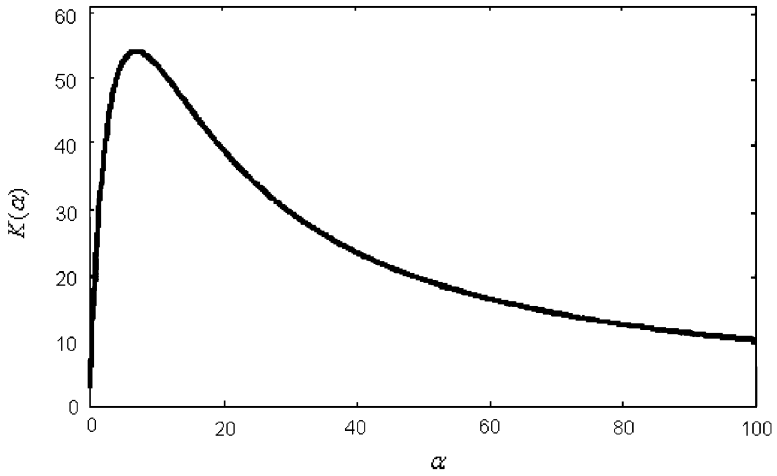


Fig. 7. Variation of $k(\alpha)$ as function of $\alpha$.

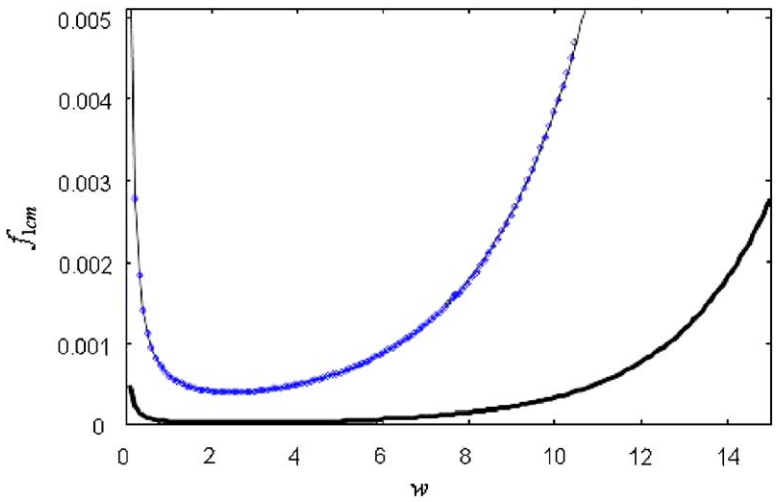


Fig. 8. The critical forcing $f_{1cm}$ for chaos control as a function of $w$ for the controlled and uncontrolled cases where $f_{11} = 0.1$, $R = 20$, $L = 0.025$. Full lines, uncontrolled case and lines with crosses, controlled case.

where the negative sign corresponds to the case of the left homoclinic orbit at $q = -q_{01s}$ and the positive sign for the right homoclinic orbit at $q = q_{01s}$. After some mathematical transformations, the quantity $k(\alpha)$ is integrated numerically (Fig. 7). For the set of parameters used in this part ($R = 20; L = 25 \times 10^{-3}$), we obtain $k(\alpha) = 2.25$. In Fig. 8 we have plotted the variation of $f_{1cm}$ versus $w$ for the controlled and uncontrolled cases. For each frequency, the limit value of $f_{1cm}$ predicted by the Melnikov theory is much larger when the electromechanical device is associated to the beam. To confirm the validity of the analytical approach, we look for the fractality of the basin of attraction. Considering first the case of the system without control and $w = 8$, a fractal structure is observed for $f = 2 \times 10^{-4}$ (Fig. 9). This value is greater than the value $f = 16 \times 10^{-5}$ calculated from the Melnikov condition (35). Figs. 9a and b are respectively obtained from Eqs. (12)–(15). Now, taking into account the presence of the control, Fig. 10 shows that for the same parameters as in Fig. 9, the fractality at $f = 2 \times 10^{-4}$ disappears when the control is added to the system. By varying $f$, the fractality

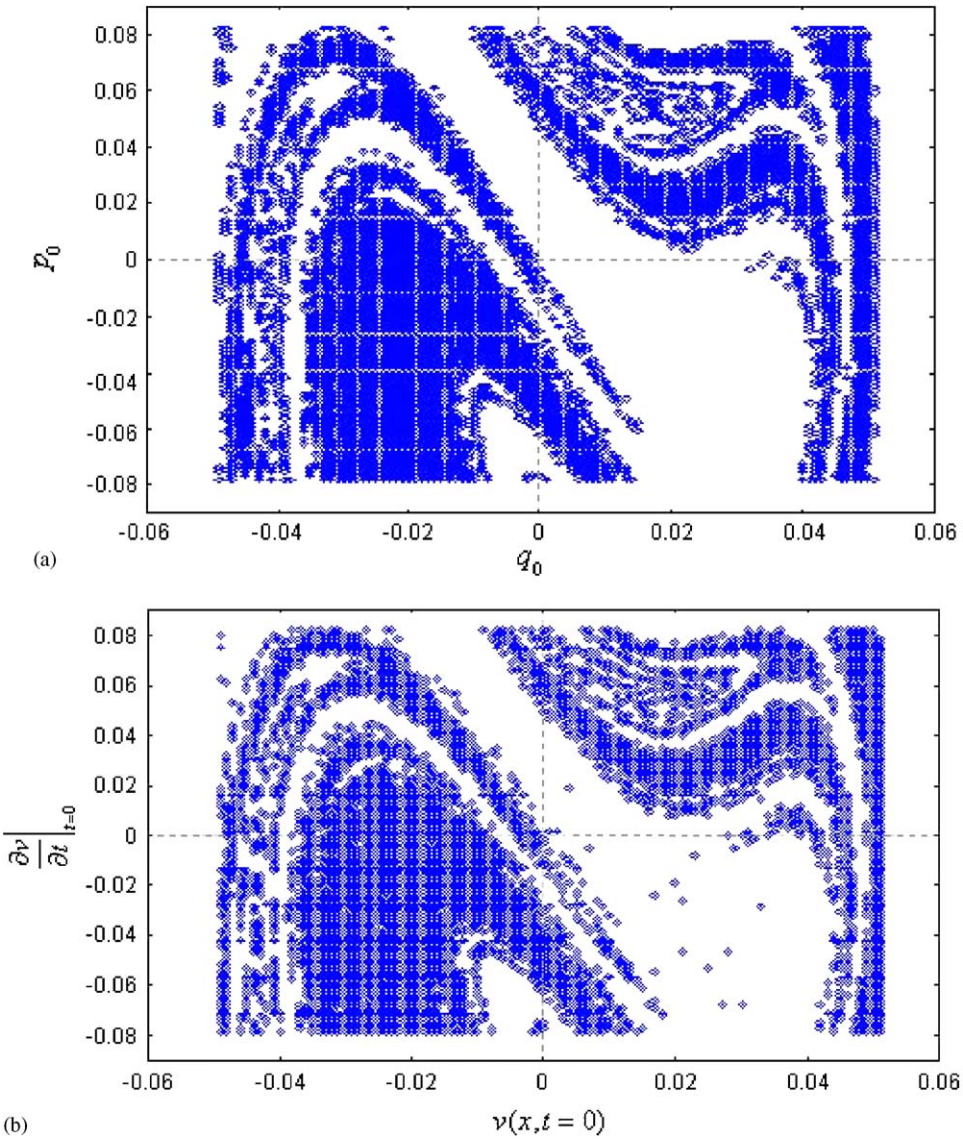


Fig. 9. Fractal basin of attraction for the uncontrolled system for $w = 8$: (a) from modal equation and (b) from partial differential equation.

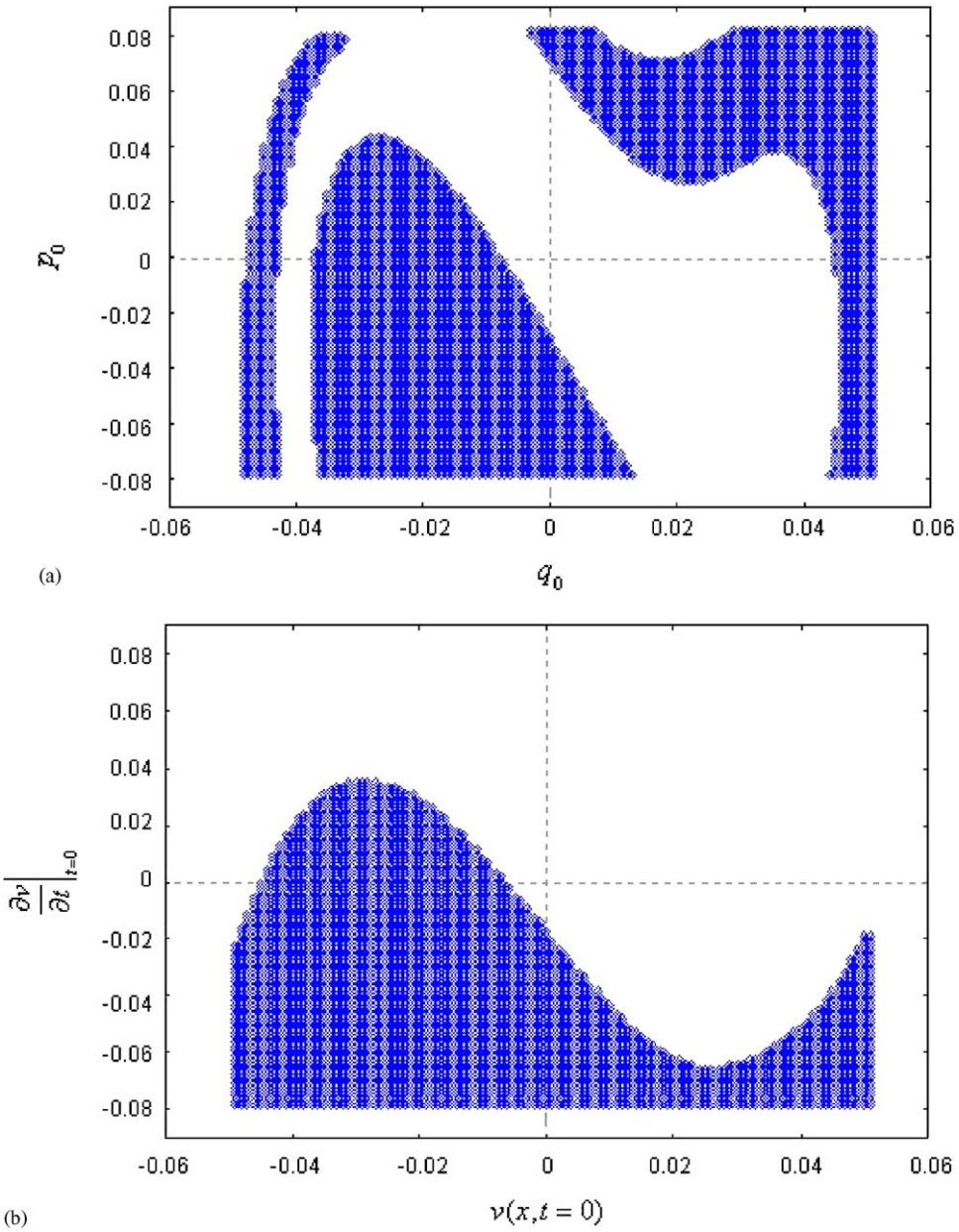


Fig. 10. Regular basin of attraction for the controlled system for $f_{11} = 0.05$, $R = 20$, $L = 0.025$, $w = 8$: (a) from modal and (b) from partial differential equation.

reappears only when $f = 5.7 \times 10^{-4}$ (Melnikov prediction). We also note that the control destabilizes the system, this justifies the difference in shapes when one compares Figs. 10a and b.

## 5. Conclusion

This paper has analyzed the electromechanical control of the beam dynamics in a state where the single-mode representation of the dynamics is that of a Duffing oscillator: control of vibration, of snap-through instability and horseshoe chaos in a beam with axial load. Analytical results have been complemented by the finite differences simulation of the full partial differential equations and the use of the Runge–Kutta algorithm

for the modal equations. The critical parameters for the reduction of amplitude, for the control of snap-through instability and for the control of chaos have been obtained from approximate analytical treatments and confirmed by the direct numerical simulation of the nonlinear partial differential equation.

## References


[1] C.R. Fuller, S.J. Eliot, P.A. Nelson, *Active Control of Vibration*, Academic Press, London, 1997.

[2] T.T.T. Song, W.F. Chen, *Active Structural Control: Theory and Practice*, Wiley, New York, 1990.

[3] R.A. Morgan, R.W. Wand, An active–passive piezoelectric absorber for structural vibration control under harmonic excitation with time-varying frequency—Part 1: algorithm development and analysis, *Journal of Vibrations and Acoustics* 124 (2002) 77–83.

[4] T. Aida, Kawazoe, S. Toda, Vibration control of plates by plate-type dynamics vibrations absorber, *Journal of Vibrations and Acoustics* 117 (1995) 332–338.

[5] T. Aida, S. Toda, S.N. Ogowa, Y. Simada, Vibration control of beams by beam type dynamics vibrations absorber, *ASCE Journal of Engineering Mechanics* 118 (1992) 163–175.

[6] L. Zhang, C.Y. Yang, M.J. Chajes, A.H.D. Cheng, Stability of active-tendon structural control with time delay, *ASCE Journal of Engineering Mechanics* 119 (1993) 1017–1024.

[7] K. Hackj, C.Y. Yang, A.H.D. Cheng, Stability, bifurcation and chaos of non-linear structure with control—I. Autonomous case, *International Journal of Non-linear Mechanics* 28 (1993) 441–454.

[8] R.J. Nagem, Madanshetty, G. Medhi, An electromechanical vibration absorber, *Journal of Sound and Vibration* 200 (4) (1997) 551–556.

[9] B.R. Nana Nbendjo, R. Tchoukuegno, P. Woafo, Active control with delay of vibration and chaos in a double-well Duffing oscillator, *Chaos, Solitons and Fractals* 18 (2003) 345–353.

[10] B.R. Nana Nbendjo, Y. Salissou, P. Woafo, Active control with delay of catastrophic motion and horseshoe chaos in a single-well Duffing oscillator, *Chaos, Solitons and Fractals* 23 (2005) 809–816.

[11] A. Nayfeh, D.T. Mook, *Nonlinear Oscillations*, Wiley, New York, 1979.

[12] P.J. Holmes, J.E. Marsden, A partial differential equation with infinitely many periodic orbits, *Archive for Rational Mechanics and Analysis* 76 (1981) 135–166.

[13] V.K. Melnikov, On the stability of the center for some periodic perturbations, *Transactions of the Moscow Mathematical Society* 12 (1963) 1–57.

[14] R. Lima, M. Pettini, Suppression of chaos by resonant parametric perturbations, *Physical Review A* 41 (1990) 726–733.

[15] L. Fronzoni, M. Gioncodo, M. Pettini, Experimental evidence of suppression of chaos by resonant parametric perturbation, *Physical Review A* 43 (1991) 6483–6487.